

Interferometric Distributed Sensing System With Phase Optical Time-Domain Reflectometry

Chen WANG^{1*}, Ying SHANG¹, Xiaohui LIU¹, Chang WANG¹,
Hongzhong WANG², and Gangding PENG³

¹Shandong Provincial Key Laboratory of Optical Fiber Sensing Technologies, Laser Institute of Shandong Academy of Sciences, Jinan, 250014, China

²Shengli Oilfield Xinsheng Geophysical Technology Co. Ltd., No. 23 Xingfu Road, Dongying, 257086, China

³School of Electrical Engineering & Telecommunications, The University of New South Wales, NSW, 2052, Australia

*Corresponding author: Chen WANG E-mail: jgwangchen@163.com

Abstract: We demonstrate a distributed optical fiber sensing system based on the Michelson interferometer of the phase sensitive optical time domain reflectometer (ϕ -OTDR) for acoustic measurement. Phase, amplitude, frequency response, and location information can be directly obtained at the same time by using the passive 3×3 coupler demodulation. We also set an experiment and successfully restore the acoustic information. Meanwhile, our system has preliminary realized acoustic-phase sensitivity around -150 dB (re rad/ μ Pa) in the experiment.

Keywords: Fiber optics sensors; Rayleigh scattering; optical time domain reflectometry; interferometry

Citation: Chen WANG, Ying SHANG, Xiaohui LIU, Chang WANG, Hongzhong WANG, and Gangding PENG, "Interferometric Distributed Sensing System With Phase Optical Time-Domain Reflectometry," *Photonic Sensors*, 2017, 7(2): 157–162.

1. Introduction

The distributed optical fiber acoustic sensors (DAS) offer the capability of measurement at thousands of points simultaneously, using a simple and unmodified optical fiber as the sensing element. It has been extensively studied and adopted for industrial applications during the past decades. Up to now, the distributed optical fiber measurements mainly include optical fiber interferometer sensors and optical backscattering based sensors. Interferometer sensors acquire distributed information by integration of the phase modulation signals, and usually two interferometers are used to determine the position, including combining the Sagnac to a Michelson interferometer [1], modified

Sagnac/Mach-Zehnder interferometer [2], twin Sagnac[3]/Michelson [4]/Mach-Zehnder [5] interferometers, and adopting a variable loop Sagnac [6]. Another distinguished technique is the use of optical backscattering based sensors. A promising technique is phase sensitive optical time domain reflectometer (ϕ -OTDR) using a narrow line-width laser [7, 8]. Brillouin-based dynamic strain sensors have been researched recently [9]. Recently, a hybrid interferometer-backscattering system is demonstrated [10], but the interferometer and the backscattering parts are working separately.

A major limitation of those distributed sensors above is that they are incapable of determining the full vector acoustic field, namely the amplitude, frequency, and phase, of the incident signal, which is

Received: 18 May 2016 / Revised: 16 October 2016

© The Author(s) 2016. This article is published with open access at Springerlink.com

DOI: 10.1007/s13320-016-0350-8

Article type: Regular

a necessity for seismic imaging. Measuring the full acoustic field is a much harder technical challenge to overcome, but in doing so, it is possible to achieve high resolution seismic imaging and also make other novel systems, for example a massive acoustic antenna.

In this paper, we demonstrate the design and characterization of a distributed optical fiber sensing system based on the Michelson interferometer of the ϕ -OTDR for acoustic measurement. Phase, amplitude, frequency response, and location information can be directly obtained at the same time. Experiments show that our system successfully restores the acoustic information and has preliminarily realized the acoustic-phase sensitivity around -150 dB (re rad/ μ Pa). Our system offers a versatile new tool for acoustic sensing and imaging, such as through the formation of a massive acoustic camera/telescope. The new technology can be used for surface, seabed, and downhole measurements all by using the same optical fiber cable.

2. Experimental setup and signal processing

The experimental setup of the Michelson interferometer of the ϕ -OTDR is shown in Fig. 1. The light source is a narrow linewidth laser with the maximum output power of 30mW and linewidth of 5 kHz. The continuous wave (CW) light with a wavelength of 1550.12 nm is injected into an acoustic-optic modulator (AOM) to generate the pulses, whose width is 200ns and the repetition rate is fixed at 20kHz. The maximum detection length is related to the repetition rate of the pulse. The time interval among the pulses should be larger than the round trip time that the pulses travel in the detection fiber to keep only one pulse inside the detection fiber. For the 20 kHz repetition rate, the detection range is around 5 km which is determined by $L < c/2nf$. The detection frequency range is also related to the repetition rate. In our case, the highest detection frequency is no more than 20 kHz theoretically.

An erbium-doped fiber amplifier (A) is used to amplify the pulses, and the ASE noise is filtered by an optical fiber Bragg grating filter (F). Then the amplified pulses are launched into a single mode detection fiber (Corning SMF-28e) by a circulator. The Rayleigh back-scattering is amplified (A) and filtered (F) again to obtain better signal-to-noise-ratio (SNR) improvement and then injected into a Michelson interferometer which consists of a circulator, a 3 \times 3 coupler, and two Faraday rotation mirrors (FRMs) [11]. The half arm length of the Michelson interferometer s is set to 5 m. The final interference signals outputting from the 3 \times 3 coupler are collected by three photodetectors (PD1–3), and then the signal processing scheme is accomplished by a software program. Theoretically, there is a 120° phase shift between two adjacent PDs. Accordingly, the outputs of the three PDs can be expressed as

$$I_k = D + I_0 \cos[\phi(t) - (k - 1) \times (2\pi/3)], \quad k = 1, 2, 3 \quad (1)$$

where $\phi(t) = \phi_s + \phi_n + \phi_0$. ϕ_s , ϕ_n , and ϕ_0 are respectively the signal to be detected, the noise, and the intrinsic phase of the system. For each point on the detection fiber, ϕ_s is obtained after the demodulation process shown in Fig. 2. It can directly demodulate all the information from the signal detected at the same time without any Fourier transforms.

In our experiment, 2000 periods for detection fiber scanning are recorded by a high-speed oscilloscope with 100 MHz sampling rate, and the total data acquisition time is 0.1 s. Here, we choose a 200 m detection fiber and several individual acoustic frequencies within the detection length and frequency range as a test example. Two piezoelectric transducer (PZT) cylinders with 10 m single mode fiber wound are put at 100 m and 160 m over 200 m detection fiber in our system as the acoustic sources. Both PZTs are driven by two function generators. To eliminate the different frequency responses of the detection fiber, we set the two function generators to output the same sine-wave with the same frequency of 200 Hz but the amplitudes are 1 V and 2 V.

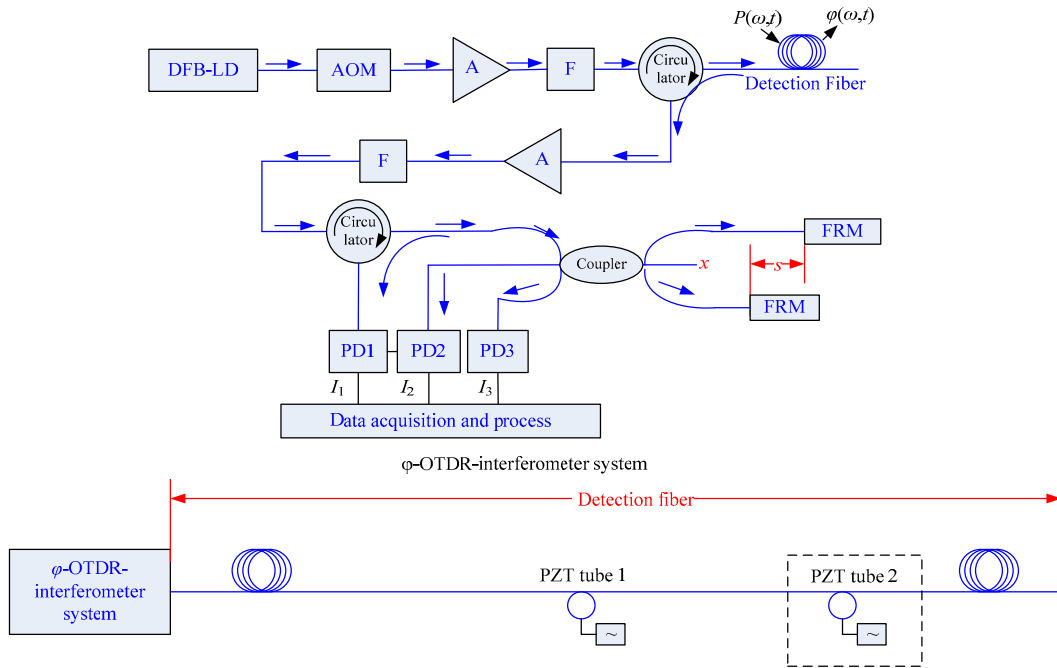


Fig. 1 Experimental setup for the Michelson interferometer of the ϕ -OTDR (DFB-FL: distributed feedback fiber laser; AOM: acoustic-optic modulator; A: erbium-doped fiber amplifier; F: optical fiber grating filter; FRM: Faraday rotation mirror; PD1–3: photodetectors; PZT: piezoelectric transducer).

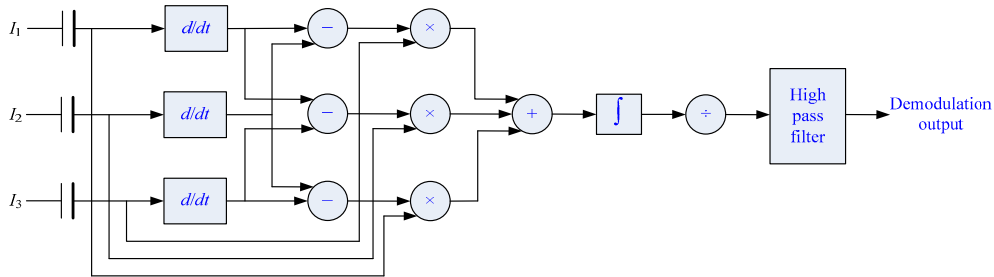


Fig. 2 Demodulation system based on the 3×3 coupler.

Figure 3(a) shows the global demodulation result. The system demodulates the whole acoustic situations along the detection fiber when both two function generators are working. We can see that besides the 1 V demodulated signal between 85 m and 105 m, our system does demodulate another signal between 155 m and 175 m. Between these two sine-like signals, there is about 50 m fiber without any vibrations in the global demodulation result, indicating no influence of the Rayleigh scatterings from different points of the detection fiber during the demodulation process. The difference of the demodulated PZT fiber position is probably caused by the change in the acquisition starting point in the oscilloscope. Figure 3(b) shows the instantaneous

frequency extracted from Fig. 3(a) at 95 m and 165 m along with their spectral analyses via fast Fourier transform (FFT) of the two demodulated signals. The amplitude of the 1 V demodulated signal at 95 m is $-0.791 \text{ dB} [=20 \lg(A_{\text{signal}}), 0.913 \text{ rad}]$, and the amplitude of the 2 V demodulated signal at 165 m is about $5.460 \text{ dB} (1.875 \text{ rad})$. The amplitude rate $A_{2V}/A_{1V}=1.875/0.913 \approx 2.054$, nearly twice between the 2 V and 1 V signal amplitudes. Also the background noise of the two demodulated signals are all around $-60 \text{ dB} [=10 \lg(A_{\text{signal}}/A_{\text{noise}}), 1 \times 10^{-3} \text{ rad}]$, so that the SNR is 29.6 dB. This result indicates that our system can well recreate the signals by their own proportions.

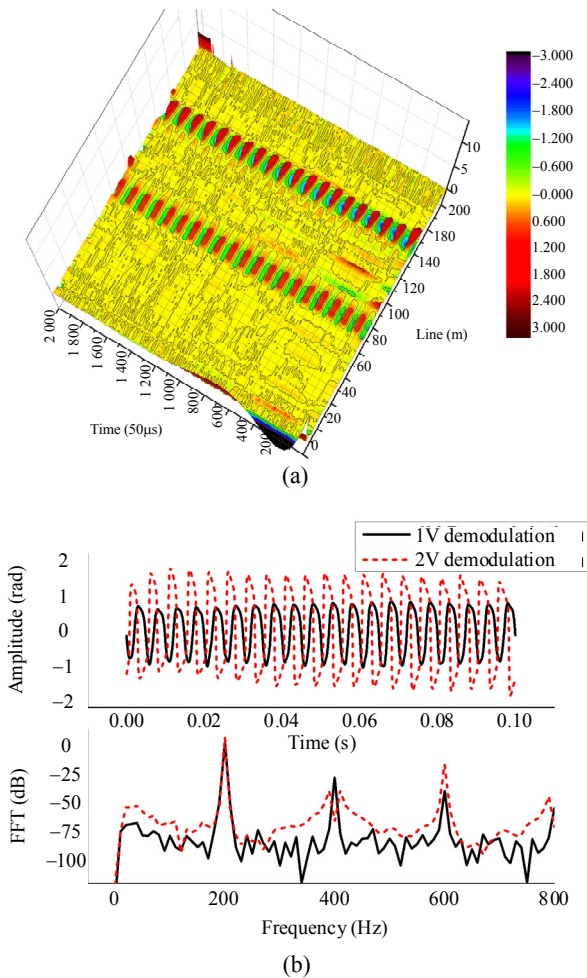


Fig. 3 Demodulated scalograms of (a) two 200Hz acoustic events, with an amplitude of 1 V at the 100 m position and an amplitude of 2 V at the 160 m position, respectively and (b) time and frequency responses of the two demodulation results.

Moreover, we use a water tank system to test the demodulation capability of our system (Fig. 4). An underwater speaker is fixed in the tank and driven by a function generator. The function generator is used to drive the underwater speaker with a 200 Hz separate sinusoidal signal. We wrap the sensing fiber into a 10 m length of fiber ring from the DAS instrument. A commercial piezoelectric hydrophone is also placed close to the fiber ring to measure the acoustic pressure amplitude. The fiber ring and the piezoelectric hydrophone are placed 5 cm away from the underwater speaker so that the sound wave produced by the speakers can be directly transmitted to the fiber.

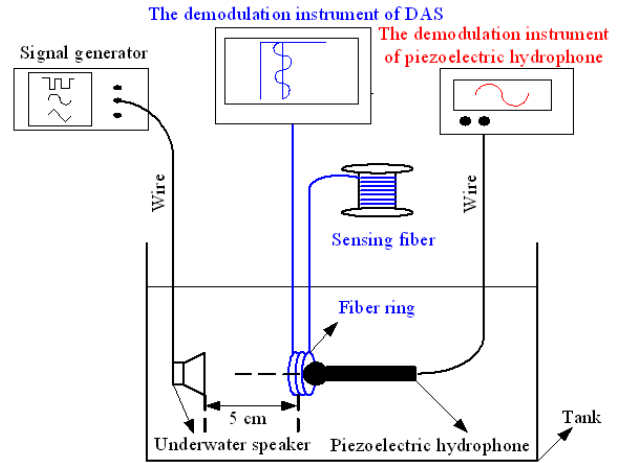


Fig. 4 Schematic diagram of underwater distributed acoustic testing experiment.

The hydrophone signal is to relate the phase measurement with acoustic pressure. So the acoustic pressure amplitudes in different acoustic intensities at 200 Hz are measured using the piezoelectric hydrophone, and the phase-pressure sensitivity of our ϕ -OTDR-interferometry system is calculated. Table 1 shows the phase-pressure data and results of our system. With a decrease in the acoustic pressure amplitudes, the demodulated phase changes also decrease. But the phase-pressure sensitivities are almost the same around 0.026 rad/Pa (-150 dB, $=20 \lg(A_{\text{signal}})$, re rad/ μ Pa), using the changed phase amplitude our system demodulated divided by the actual acoustic pressure amplitude the piezoelectric hydrophone detected, indicating that our system can well demodulate the amplitude, frequency, and phase of the acoustic signals with a sensitivity of -150 dB.

Table 1 Experimental data of sensitivity.

Piezoelectric hydrophone		DAS	
Amplitude (mV)	Acoustic pressure (Pa)	Phase changes (rad)	Acoustic phase sensitivity dB (re rad/ μ Pa)
30	15	0.654	-147
24	12	0.312	-152
18	9	0.243	-151
12	6	0.154	-151

3. Further discussion

Another point that should be explained is that due to the participation of the interferometer the width of the source demodulated by our ϕ -OTDR-interferometer system is broadened than its origin. The extended length between the original source and the demodulated one equals just to the length of the arm length of the interferometer. On the contrary, the introduction of the Michelson interferometer has its advantage to the signal demodulation and could improve the sensitivity of our system because the effective detecting fiber is expanded. It could increase the dynamic sensitivity of our system significantly. These parameters should be chosen wisely in real applications. The polarization of the Rayleigh backscattering is also important to our system. The advantage of using Michelson interferometer rather than Mach-Zehnder one is that the FRMs keep the polarization states of the input and output lights independent from the fiber birefringence. And also the interferometer is not used as the sensing fiber, so the polarization is not a critical issue. Further experiment will be done to eliminate the polarization influence with certain polarizer at the beginning of the detection fiber.

In application, the mapping of acoustic events is very important, which directly gives what is happening around the detecting area. Classically, point sensors have been used as a serial of arrays to determine when, what, and where the acoustic event is, thus making a high cost of the monitor. Distributed sensors are much cheaper but have a major limitation that they are incapable of determining the full vector acoustic field, namely the amplitude, frequency, and phase, of the incident signal, which is a necessity for seismic imaging. By using the method of our ϕ -OTDR interferometry, it offers a versatile new tool for acoustic mapping and imaging in one single optical fiber, such as through the formation of a massive acoustic camera/telescope. For example, it is possible to incorporate our system as the optical hydrophone or

directional accelerometer arrays and even to measure on existing arrays directly with the appropriate wavelength choice. It also can be used in many seismic acquisitions to date, encompassing vertical seismic profiling, in both flowing and non-flowing wells, and surface seismic surveys.

4. Conclusions

In this paper, we demonstrate the design and characterization of a distributed optical fiber sensing system based on the Michelson interferometer of the ϕ -OTDR for acoustic measurement. The phase, amplitude, frequency response, and location information can be directly obtained at the same time by using the passive 3×3 coupler demodulation. Experiments show that our system successfully restores the acoustic information with the acoustic-phase sensitivity around -150 dB (re rad/ μ Pa). Our system offers a versatile new tool for acoustic sensing and imaging, such as through the formation of a massive acoustic camera/telescope. The new technology can be used for surface, seabed, and downhole measurements. The use of the system in downhole applications allows a continuum of benefits extending to flow profiling and condition monitoring, all using the same optical fiber cable.

Acknowledgment

This work was supported by the Shandong Natural Science Foundation (No. ZR2013FL028), Science and Technology Development Project of Shandong Province (2014GGX103019), and Innovation and Achievement Transformation Projects of Shandong Province (2014ZZCX04206).

Open Access This article is distributed under the terms of the Creative Commons Attribution 4.0 International License (<http://creativecommons.org/licenses/by/4.0/>), which permits unrestricted use, distribution, and reproduction in any medium, provided you give appropriate credit to the original author(s) and the source, provide a link to the Creative Commons license, and indicate if changes were made.

References

- [1] S. J. Spammer, P. L. Swart, and A. A. Chtcherbakov, "Merged Sagnac-Michelson interferometer for distributed disturbance detection," *Journal of Lightwave Technology*, 1997, 15(6): 972–976.
- [2] A. A. Chtcherbakov, P. L. Swart, S. J. Spammer, and B. M. Lacquet, "Modified Sagnac/Mach-Zehnder interferometer for distributed disturbance sensing," *Microwave and Optical Technology Letters*, 1999, 20(1): 34–36.
- [3] S. J. Russell, K. R. C. Brady, and J. P. Dakin, "Real-time location of multiple time-varying strain disturbances acting over a 40 km fiber section using a novel dual-Sagnac interferometer," *Journal of Lightwave Technology*, 2001, 19(2): 205–213.
- [4] X. Hong, J. Wu, C. Zuo, F. Liu, H. Guo, and K. Xu, "Dual Michelson interferometers for distributed vibration detection," *Applied Optics*, 2011, 50(22): 4333–4338.
- [5] Q. Sun, D. Liu, J. Wang, and H. Liu, "Distributed fiber-optic vibration sensor using a ring Mach-Zehnder interferometer," *Optics Communications*, 2008, 281(6): 1538–1544.
- [6] X. J. Fang, "Fiber-optic distributed sensing by a two-loop Sagnac interferometer," *Optics Letters*, 1996, 21(6): 444–446.
- [7] J. C. Juarez, E. W. Maier, K. N. Choi, and H. F. Taylor, "Distributed fiber-optic intrusion sensor system," *Journal of Lightwave Technology*, 2005, 23(6): 2081–2087.
- [8] J. C. Juarez and H. F. Taylor, "Field test of a distributed fiber-optic intrusion sensor system for long perimeters," *Applied Optics*, 2007, 46(11): 1968–1971.
- [9] Y. Dong, L. Chen, and X. Bao, "Time-division multiplexing-based BOTDA over 100 km sensing length," *Optics Letters*, 2011, 36(2): 277–279.
- [10] T. Zhu, Q. He, X. Xiao, and X. Bao, "Modulated pulses based distributed vibration sensing with high frequency response and spatial resolution," *Optics Express*, 2013, 21(3): 2953–2963.
- [11] M. D. Todd, M. Seaver, and F. Bucholtz, "Improved, operationally-passive interferometric demodulation method using 3×3 coupler," *Electronics Letters*, 2002, 38(15): 784–786.